Japanese Journal of Applied Physics

REGULAR PAPERS

Effects of SF_6 plasma treatment on the properties of InGaZnO thin films

Japanese Journal of Applied Physics **57**, 03DA01 (2018)
https://doi.org/10.7567/JJAP.57.03DA01

REGULAR PAPER

Effects of SF_6 plasma treatment on the properties of InGaZnO thin films

Jinsung Choi[1], Byung Seong Bae[2], and Eui-Jung Yun[3*]

[1]*Department of NanoBioTronics, Hoseo University, Asan, Chungnam 31499, Republic of Korea*
[2]*Department of Display Engineering, Hoseo University, Asan, Chungnam 31499, Republic of Korea*
[3]*Department of ICT Automotive Engineering, Hoseo University, Dangjin, Chungnam 31702, Republic of Korea*

*E-mail: ejyun@hoseo.edu

Received July 18, 2017; accepted August 30, 2017; published online January 9, 2018

The effects of sulfur hexafluoride (SF_6) plasma on the properties of amorphous InGaZnO (a-IGZO) thin films were examined. The properties of the a-IGZO thin films were characterized by Hall effect measurement, dynamic secondary ion mass spectroscopy (SIMS), and X-ray photoelectron spectroscopy (XPS). The IGZO thin films treated with SF_6 plasma before annealing had a very high resistance mainly owing to the inclusion of S into the film surface, as evidenced by SIMS profiles. On the other hand, the samples treated with SF_6 plasma after annealing showed better electrical properties with a Hall mobility of 10 $cm^2/(V{\cdot}s)$ than the untreated samples or the samples SF_6 plasma-treated before annealing. This was attributed to the increase in the number of oxygen vacancy defects in the a-IGZO thin films owing to the enhanced out-diffusion of O to the ambient and the increase in the number of F-related donor defects originating from the incorporation of a much larger amount of F than of S into the film surface, which were confirmed by XPS and SIMS.

1. Introduction

Recently, amorphous indium–gallium–zinc oxide (a-IGZO) thin films have attracted considerable attention as an active layer of thin-film transistors (TFTs) for the application of active-matrix flat-panel displays (AMFPDs).[1–17] Fluorine (F) reduced the number of oxygen vacancies and electron traps in the IGZO or tin-oxide (SnO) channel layers existing at an energy level close to the valence band maximum, which played a positive role in the stability and electrical properties of a-IGZO or SnO TFTs.[18–21]

On the other hand, sulfur (S) inclusion would produce in-band gap defects, trap electrons, and result in a very high resistance similar to those in amorphous chalcogenide cases, which had negative effects on the electrical properties of a-IGZO thin films.[22] In our previous paper, we reported that S incorporation played a positive role in the electrical properties and stabilities of sulfur-incorporated zinc-tin-oxide TFTs.[23] Hence, there seems to be a discrepancy with the effects of S inclusion on the properties of oxide semiconductor thin films. Therefore, in this study, the effects of the incorporation of F and S on the properties of a-IGZO thin films were examined by SF_6 plasma treatment.

This paper is an extended version of the AM-FPD'17 Conference proceedings paper.[24] In the present paper, new data, such as those in Figs. 1(a)–1(c) and 1(e), 2, 3(a), and 4 and 5, are included. The new data for the samples treated with SF_6 plasma before annealing were also added to Table I. From the results of more comprehensive analyses of the new data, more in-depth considerations and new interpretations of the experimental results were made.

2. Experimental methods

50-nm-thick a-IGZO thin films were deposited on SiO_2 substrates at 200 °C using an IGZO sputtering target under the following conditions: a radio frequency (RF) power of 50 W, a working pressure of 5 mTorr, and an O_2 ratio of 25%. The a-IGZO thin films were annealed at 400 °C for 1 h in air after deposition. To examine the effects of heat and SF_6 treatments on the properties of the samples, the IGZO thin films were treated with SF_6 plasma before or after annealing using reactive ion etching (RIE) equipment under the following conditions: a flow rate of 20 cm^3/min, an RF power of 180 W, and a treatment time range of 0 to 60 s.

The contents (at. %) and chemical bonding states of In, Ga, Zn, and O in the IGZO thin films were analyzed by X-ray photoelectron spectroscopy (XPS). The changes in the depth profiles of In, Ga, Zn, and O in the samples were examined by dynamic secondary ion mass spectroscopy (D-SIMS). The electrical properties of the IGZO thin films were characterized by Hall effect measurement.

3. Results and discussion

3.1 Hall measurement analysis

Table I lists the Hall effect measurement results, which revealed the electrical properties of a series of samples prepared in this study. We observed from the Hall measurement results that regardless of the SF_6 plasma treatment, the samples without annealing showed the insulator behavior. However, the untreated samples which were annealed, exhibited semiconductor characteristics (see the first column in Table I). This suggests that annealing is necessary to improve the electrical properties of the samples. Furthermore, we believe that the initial state of the sample surface is very important for the SF_6 treatment to be effective. Therefore, it is important to compare the effects of the treatment before and after annealing. As indicated in Table I, the IGZO thin films treated with SF_6 plasma prior to annealing exhibited a very high resistance, whereas those treated after annealing showed improved electrical properties.

The diffusion of S into the IGZO films produced in-band gap defects and caused a very high resistance.[22] This suggests that the high resistance of the samples treated with SF_6 plasma before annealing is related to the introduction of S into the samples. Note that the metal elements in the IGZO films can react with S, resulting in a decrease in the number of oxygen vacancy (V_o) donor defects, which causes a decrease in electron concentration and an increase in resistance.

For the samples treated after annealing, the product of the mobility (μ) and carrier concentration (n) increased with increasing SF_6 plasma treatment time, resulting in a decrease in resistivity (ρ) (Table I). This result followed the equation

Table I. Summary of the Hall measurement results for the series of samples prepared in this study.

Sample description	Resistivity (Ω·cm)	Hall mobility [$cm^2/(V{\cdot}s)$]	Carrier concentration ($1/cm^3$)
IGZO films untreated with SF_6 plasma	0.156	7.75	5.16×10^{18}
IGZO films treated with SF_6 for 30 s before annealing	Immeasurable owing to very high resistance		
IGZO films treated with SF_6 for 45 s before annealing	Immeasurable owing to very high resistance		
IGZO films treated with SF_6 for 30 s after annealing	0.068	10	9.14×10^{18}
IGZO films treated with SF_6 for 45 s after annealing	0.083	6.83	1.1×10^{19}

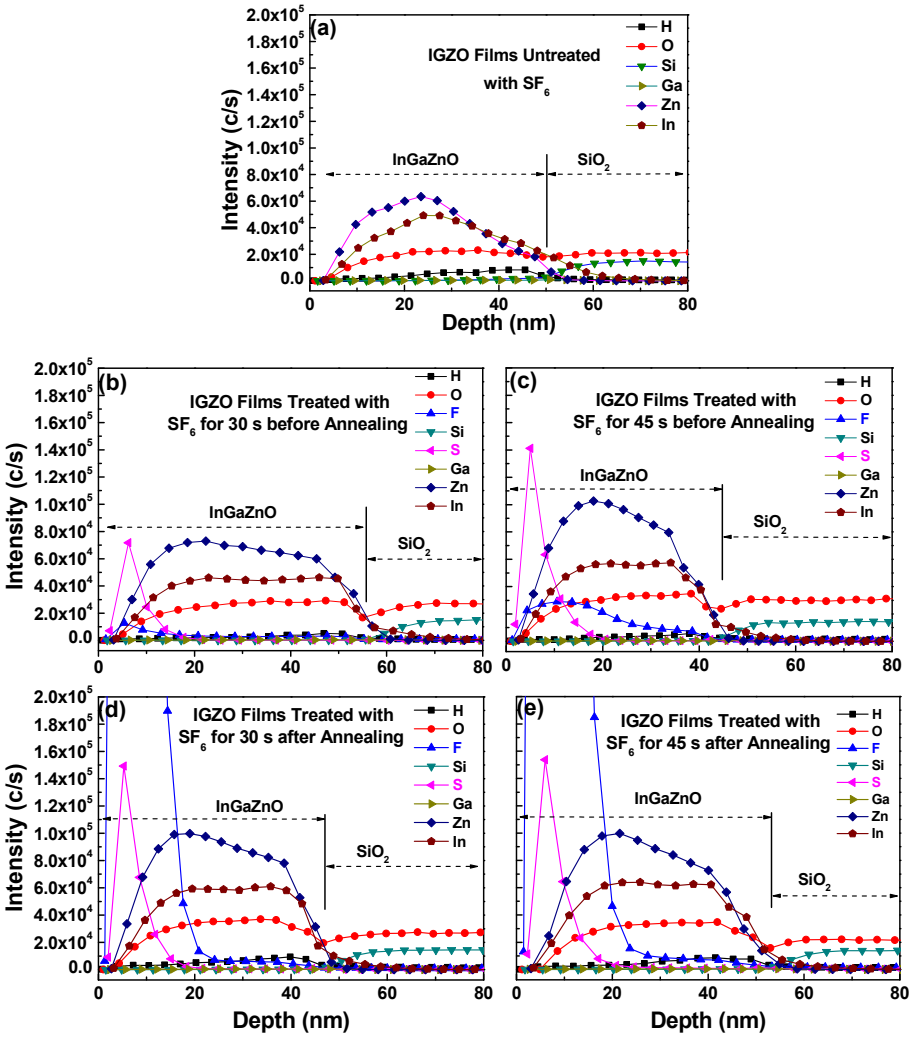

Fig. 1. (Color online) Intensity variations in the hydrogen (H), oxygen (O), fluorine (F), silicon (Si), sulfur (S), gallium (Ga), zinc (Zn), and indium (In) concentrations in the IGZO thin films (a) untreated, treated with SF_6 plasma for (b) 30 and (c) 45 s before annealing, and treated with SF_6 plasma for (d) 30 and (e) 45 s after annealing, which were obtained from the SIMS depth profiles. (d) was reproduced with permission from Ref. 24. © 2017 FTFMD.

$$\rho = \frac{1}{nq\mu}, \tag{1}$$

where q is the charge of an electron. Table I shows that the improvement of the electrical properties of the SF_6 plasma-treated samples after annealing is closely associated with the diffusion of F into the sample surfaces.

3.2 SIMS analysis

The SIMS depth profiles shown in Fig. 1 exhibit typical intensity variations in H, O, F, S, Si, Ga, Zn, and In concentrations in the IGZO thin films treated with SF_6 plasma for 0–45 s before or after annealing. As shown in Fig. 1, in the case of the samples treated with SF_6 plasma before annealing, the SF_6 plasma treatment caused the diffusion of S at a much higher concentration than F into the sample surface. This supports the Hall measurement result in that the high resistance of the samples treated with SF_6 plasma before annealing is mainly due to the introduction of S into the samples.

On the other hand, as shown in Fig. 1, in the case of the samples treated with SF_6 plasma after annealing, a large amount of F diffused into the IGZO surface after the SF_6 plasma treatment. Therefore, the increased F concentration apparently causes an increase in the number of F-related donor defects. Consequently, the electron concentration in the IGZO films increased, which in turn resulted in the

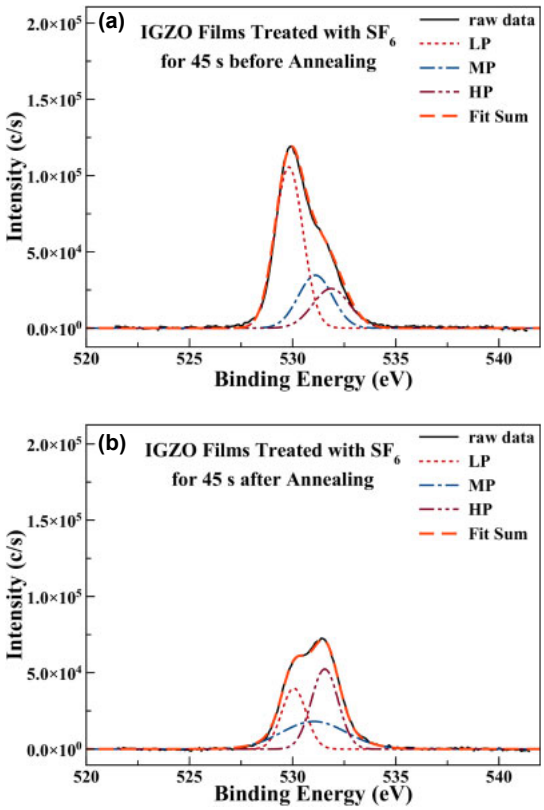

Fig. 2. (Color online) Typical O 1s narrow-scan XPS spectra fitted using three LP, MP, and HP Gaussian peaks for the IGZO thin films treated with SF_6 plasma for 45 s (a) before and (b) after annealing.

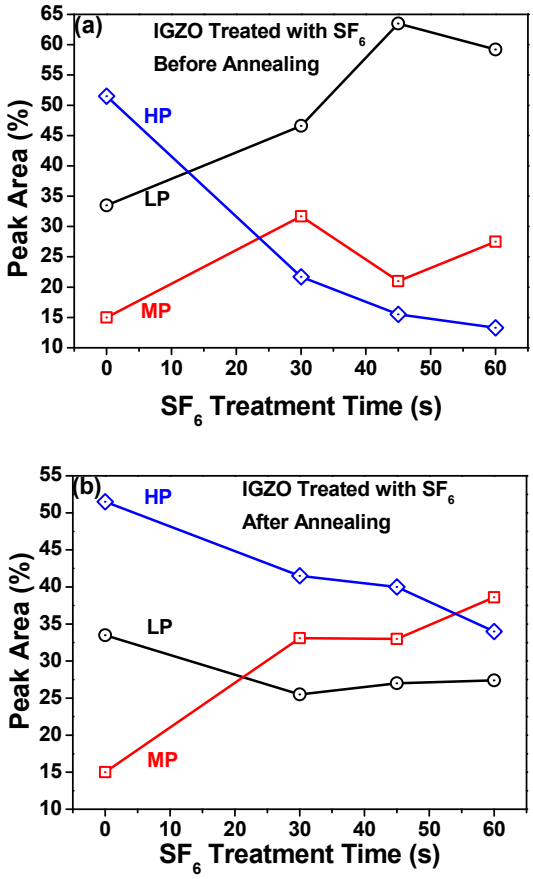

Fig. 3. (Color online) Percentage area characteristics of three Gaussian peaks as a function of the SF_6 plasma treatment time obtained from the O 1s narrow scan XP spectra of IGZO thin films treated with SF_6 plasma (a) before and (b) after annealing. This result was obtained after fitting the O 1s peaks using the three LP, MP, and HP Gaussian peaks, as shown in Fig. 2. (b) was reproduced with permission from Ref. 24. © 2017 FTFMD.

decrease in resistivity in the case of the samples treated with SF_6 plasma after annealing, as evidenced by Table I. Figure 1 shows that the concentration of F in the samples treated with SF_6 plasma after annealing was much higher than that in the samples treated with SF_6 plasma before annealing. This discrepancy in F concentration was attributed to the decrease in the amount of F due to the out-diffusion of F from the samples into the ambient during annealing.

3.3 XPS analysis

All binding energies obtained by XPS were calibrated using the C 1s reference peak at 284.6 eV. The O 1s narrow-scan XP spectra of the IGZO thin films were fitted using three Gaussian peaks associated with the low, middle, and high peaks (LP, MP, and HP) centered at approximately 529.81–530.06, 531.03–531.1, and 531.55–531.87 eV, respectively. The LP is associated with O^{2-} ions surrounded by In, Ga, and Zn metal atoms in a fully oxidized stoichiometric IGZO system. The MP can also be attributed to O^{2-} ions in the oxygen-deficient regions within the IGZO matrix and is related to V_o defects, whereas the HP is related to the chemisorbed or dissociated oxygen or to O–H bonding near the film surface.[15–17,19,25–30]

Figures 2(a) and 2(b) present typical examples of the O 1s narrow-scan XP spectra fitted using the LP, MP, and HP Gaussian peaks in the samples treated with SF_6 plasma for 45 s before and after annealing, respectively. The fitting of the O 1s peaks using the three LP, MP, and HP Gaussian peaks was excellent. As shown in Fig. 2(a), for IGZO films treated with SF_6 plasma for 45 s before annealing, the percentage areas of LP centered at approximately 529.81 eV, MP at 531.1 eV, and HP at 531.87 eV were 63.5, 21, and 15.5%, respectively. On the other hand, Fig. 2(b) shows that the percentage areas of LP centered at approximately 530.06 eV, MP at 531.03 eV, and HP at 531.55 eV were 27, 33, and 40%, respectively, for the IGZO thin films treated with SF_6 plasma for 45 s after annealing.

Figures 3(a) and 3(b) also show the percentage areas of the three Gaussian peaks as a function of the SF_6 plasma treatment time for the samples treated with SF_6 before and after annealing, respectively, which were obtained after fitting the O 1s peaks using the three LP, MP, and HP Gaussian peaks, as shown in Fig. 2. For the samples treated with SF_6 plasma before annealing [see Fig. 3(a)], the LP area increased with increasing SF_6 plasma treatment time, which suggests that the in-diffusion of O from the ambient to the sample surface accelerates during the SF_6 and/or annealing treatments, as shown in Figs. 1(b) and 1(c). On the other hand, the HP area decreased rapidly with increasing SF_6 plasma treatment time, indicating that a longer SF_6 plasma treatment time removes a higher amount of O or H near the sample surfaces effectively before annealing. Figure 3(a) also shows that the MP area fluctuates between 21 and 32% with increasing treatment time. The decrease in MP area between 30 and 45 s was related to the decrease in V_o owing to the annihilation of V_o by the in-diffused O and S.

As indicated in Fig. 3(b), in the case of the samples treated with SF_6 plasma after annealing, the LP area decreased after

the SF_6 plasma treatment, which suggests that the metal oxide bonds reacted with S–F_x or F radicals, as evidenced in Figs. 1(d) and 1(e), and the out-diffusion of O from the film into the ambient occurred. The HP area also decreased with increasing treatment time, suggesting that the amount of O or H appears to decrease linearly near the surfaces of the SF_6 plasma-treated IGZO thin films. The MP area increased with increasing SF_6 plasma treatment time. Therefore, when the IGZO thin films were treated with SF_6 plasma after annealing, the number of oxygen vacancies increased, indicating that the out-diffusion of O from the film into the ambient increases with increasing SF_6 plasma treatment time, which causes an increase in carrier concentration, as confirmed in the samples treated with SF_6 plasma for 30 and 45 s from the Hall measurement results.

Figure 4 shows the analyzed contents (at. %) of the samples treated with SF_6 plasma after annealing, which were obtained by XPS. As shown in Fig. 4, O contents (at. %) were 68, 63, 62, and 61 for the SF_6 plasma treatment times of 0, 30, 45, and 60 s, respectively. This confirmed that with increasing SF_6 plasma treatment time, the O content decreased owing to the out-diffusion of O from the samples. Therefore, a longer SF_6 plasma treatment time enhances the formation of V_o donor defects in the films. The large decrease in O content occurred at the initial stage of treatment (in the range of 0–30 s) while the small decrease in O content occurred at the next stage of treatment (in the range of 30–60 s). This trend in the decrease in O content corresponds to the XPS results in Fig. 3(b) in that the increase in MP area % became smaller in the samples treated with SF_6 plasma after annealing. This supports the main findings in Fig. 3(b) in that the number of oxygen vacancies in the samples treated with SF_6 plasma after annealing increased owing to the enhancement of the out-diffusion of O from the film into the ambient with increasing SF_6 plasma treatment time.

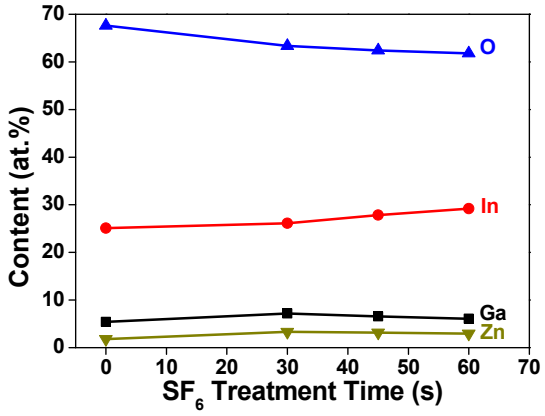

Fig. 4. (Color online) Variations in element contents (at. %) with the SF_6 plasma treatment time for the IGZO thin films treated with SF_6 plasma after annealing.

Figure 5 shows the S 2p and F 1s narrow scan XP spectra of a series of samples treated with SF_6 plasma for 30 and 45 s before and after annealing. As shown in Figs. 5(a) and 5(b), for all IGZO thin films treated with SF_6 plasma, one dominant S 2p peak was observed at 160 eV, which was assigned to S^{2-}.[31] This confirms that the included S^{2-} ions would react with In, Ga, and Zn metal atoms, which results in a decrease in the number of V_o donor defects and explains the high resistance of the samples treated with SF_6 plasma before annealing. As shown in Figs. 5(c) and 5(d), the F 1s peak at 684 eV was observed in the samples treated with SF_6 plasma after annealing, whereas the same peak was not detected in the samples treated before annealing, supporting the SIMS

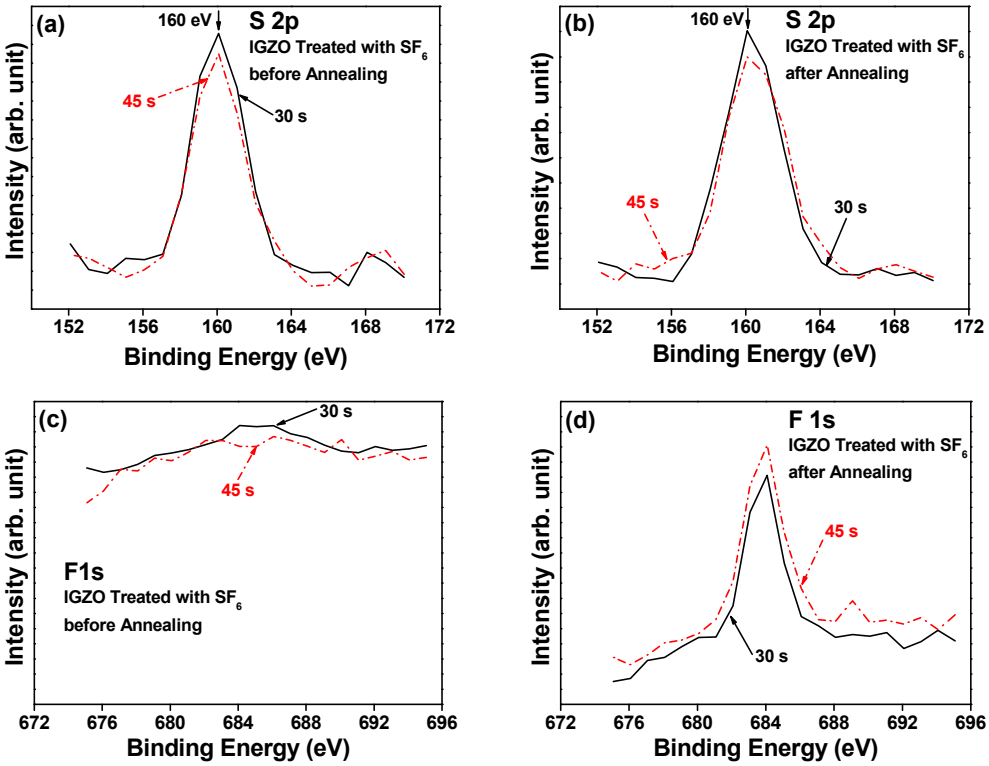

Fig. 5. (Color online) S 2p narrow-scan XP spectra of the IGZO films treated with SF_6 plasma for 30 and 45 s (a) before and (b) after annealing. F 1s narrow-scan XP spectra of the IGZO films treated with SF_6 plasma for 30 and 45 s (c) before and (d) after annealing.

result indicating that the SF_6 plasma-treated samples after annealing contain a much higher F concentration than those before annealing. Therefore, the higher F concentration gives rise to the formation of more F-related donor defects. Accordingly, it increases the electron concentration in the samples, decreasing the resistivity of the samples treated with SF_6 plasma after annealing.

Interestingly, the F diffusion can suppress the inclusion of S into the V_o donor defect sites for the samples treated with SF_6 plasma after annealing using the following arguments: Both samples treated with SF_6 plasma before or after annealing show a significant amount of diffused S owing to the SF_6 treatment (based on SIMS results in Fig. 1 and XPS results in Fig. 5). The main difference is the much greater F diffusion and higher conductivity in the samples SF_6 plasma-treated after annealing than in the samples SF_6 plasma-treated before annealing. Furthermore, a much larger increase in F concentration than in S concentration was observed in the samples SF_6 plasma-treated after annealing, as shown in Fig. 1. At a high F content, the doped F atoms may form F–metal complexes (F inclusion into V_o defects), F–O defects (F-induced V_o donor defects), and interstitial F (F_i) defects. Increasing the F content allows more chances for the F atoms to occupy the substitutional O sites (F_O) than for the S atoms to occupy the O sites (S_O) during the SF_6 plasma treatment owing to the smaller ionic radius of F (0.64 Å) than of S (1.04 Å) and O (0.66 Å),[32] which induces the inclusion of F into the V_o defects and leads to the suppression of S inclusions into the V_o donor defect sites for the samples SF_6 plasma-treated after annealing. This inclusion of F into the V_o defects suggests that some of the F atoms occupy V_o defects, as reported previously.[18–21] This suggests that the V_o defect concentration decreases, resulting in an increase in the resistivity of the samples. In this case, however, the V_o defect concentration increased and the resistivity decreased in the samples SF_6 plasma-treated after annealing with a large number of F atoms. Therefore, a higher F concentration causes another dominant mechanism, such as the formation of more F-related donor defects, which is related to F-induced V_o defects. In the case of the samples SF_6 plasma-treated after annealing, the LP area decreased and the out-diffusion of O from the film into the ambient increased with increasing SF_6 plasma treatment time, suggesting that these samples were exposed to harsh conditions with many defects. This explains why the F atoms form preferentially more F-related donor defects instead of occupying oxygen vacancies.

In addition, the interaction between F and S can occur, even though separate mechanism arguments were used in the main text, where a much larger number of F-related donor defects had a larger effect on the conductivity. This is because the reaction between F and S can take place easily in an exothermic process because the standard enthalpy of the formation of SF_6 at room temperature and 1 atm would be highly negative (−1209 kJ/mol).[33] Further research to address this issue in detail is currently under way.

The full width at half maximum (FWHM) values of the deconvoluted MP components for the samples treated with SF_6 plasma for 30, 45, and 60 s before annealing were determined from XPS results to be 1.95, 1.95, and 1.81 eV, respectively. On the other hand, those for the samples treated for 30, 45, and 60 s after annealing were 3.48, 3.69, and 3.07 eV, respectively. These results suggest that the increase in the FWHM of MP occurred in all samples treated with SF_6 plasma after annealing. The FWHM is determined by various factors, such as natural line width, rough sample surface, chemical interaction, preferable crystalline surface structure, crystalline sample structure, and the distribution of different physiochemicals around the site from which the signal originates. Therefore, we suggest that the increase in the FWHM of MP in the samples treated with SF_6 plasma after annealing is mainly due to the changes in the binding energy distribution of O^{2-} ions in the oxygen-deficient regions within the IGZO matrix resulting from the SF_6 plasma treatment, and that the increase in FWHM can also be suppressed by annealing.

4. Conclusions

In this study, the effects of the inclusion of F and S atoms on the properties of a-IGZO thin films through a SF_6 plasma treatment were examined. For the samples treated with SF_6 plasma before annealing, (1) the observed high resistance was attributed to the decrease in the number of V_o donor defects due to the reaction of the introduced S with metal elements and (2) the longer SF_6 plasma treatment time removes a higher amount of O or H near the sample surfaces effectively before annealing. In the case of the samples treated with SF_6 plasma after annealing, the product of the mobility and carrier concentration increased with increasing SF_6 plasma treatment time, resulting in a decrease in the resistivity of the samples. SIMS and XPS confirmed that the increased F concentration in the samples caused an increase in the number of F-related donor defects. Consequently, the electron concentration in the IGZO thin films increased. The number of oxygen vacancies in the samples treated with SF_6 plasma after annealing also increased. This resulted from the enhanced out-diffusion of O from the film into the ambient during the treatment, which in turn gave rise to an increase in carrier concentration.

Acknowledgment

This research was supported by the Basic Science Research Program through the National Research Foundation of Korea (NRF) funded by the Ministry of Education (NRF-2016R1D1A3B03932570).

1) T. Moriga, D. R. Kammler, and T. O. Mason, J. Am. Ceram. Soc. **82**, 2705 (1999).
2) M. Orita, H. Tanji, M. Mizuno, H. Adachi, and I. Tanaka, Phys. Rev. B **61**, 1811 (2000).
3) K. Nomura, H. Ohta, K. Ueda, T. Kamiya, M. Hirano, and H. Hosono, Science **300**, 1269 (2003).
4) T. Kamiya and H. Hosono, Int. J. Appl. Ceram. Technol. **2**, 285 (2005).
5) K. Nomura, T. Kamiya, H. Ohta, T. Uruga, M. Hirano, and H. Hosono, Phys. Rev. B **75**, 035212 (2007).
6) S. P. Chang, Y. W. Song, S. G. Lee, S. Y. Lee, and B. K. Ju, Appl. Phys. Lett. **92**, 192104 (2008).
7) Y. Shimura, K. Nomura, H. Yanagi, T. Kamiya, M. Hirano, and H. Hosono, Thin Solid Films **516**, 5899 (2008).
8) K. Abe, N. Kaji, H. Kumomi, K. Nomura, T. Kamiya, M. Hirano, and H. Hosono, IEEE Trans. Electron Devices **58**, 3463 (2011).
9) J. Jeong, J. Kim, G. J. Lee, and B.-D. Choi, Appl. Phys. Lett. **100**, 023506 (2012).
10) J. Jeong, G. J. Lee, J. Kim, S. M. Jeong, and E. J.-H. Kim, J. Appl. Phys. **114**, 094502 (2013).

11) M. Mativenga, S. An, S. Lee, J. Um, D. Geng, R. K. Mruthyunjaya, G. N. Heiler, and T. J. Tredwell, IEEE Trans. Electron Devices **61**, 2106 (2014).
12) E. T. Kim, C.-K. Kim, M. K. Lee, T. W. Bang, Y.-K. Choi, S.-H. K. Park, and K. C. Choi, Appl. Phys. Lett. **108**, 182104 (2016).
13) L. Petti, N. Münzenrieder, C. Vogt, H. Faber, L. Büthe, G. Cantarella, F. Bottacchi, T. D. Anthopoulos, and G. Tröster, Appl. Phys. Rev. **3**, 021303 (2016).
14) X. Ding, F. Huang, S. Li, J. Zhang, X. Jiang, and Z. Zhang, Electron. Mater. Lett. **13**, 45 (2017).
15) C.-H. Hung, S.-J. Wang, P.-Y. Liu, C.-H. Wu, H.-P. Yan, N.-S. Wu, and T.-H. Lin, Mater. Sci. Semicond. Process. **67**, 84 (2017).
16) H. Xie, J. Xu, G. Liu, L. Zhang, and C. Dong, Mater. Sci. Semicond. Process. **64**, 1 (2017).
17) M.-H. Kim, M.-J. Choi, K. Kimura, H. Kobayashi, and D.-K. Choi, Solid-State Electron. **126**, 87 (2016).
18) J. P. Bermundo, Y. Ishikawa, H. Yamazaki, T. Nonaka, M. N. Fujii, and Y. Uraoka, Appl. Phys. Lett. **107**, 033504 (2015).
19) Y.-H. Joo and C.-I. Kim, Thin Solid Films **583**, 40 (2015).
20) M. Furuta, J. Jiang, M. P. Hung, T. Toda, D. Wang, and G. Tatsuoka, ECS J. Solid State Sci. Technol. **5**, Q88 (2016).
21) P.-C. Chen, Y.-C. Chiu, Z.-W. Zheng, C.-H. Cheng, and Y.-H. Wu, J. Alloys Compd. **707**, 162 (2017).
22) J. Kim, H. Hiramatsu, H. Hosono, and T. Kamiya, J. Ceram. Soc. Jpn. **123**, 537 (2015).
23) S.-A. Oh, K. M. Yu, S.-H. Jeong, B. S. Bae, and E.-J. Yun, J. Korean Phys. Soc. **66**, 1144 (2015).
24) J. Choi, B. S. Bae, and E.-J. Yun, Proc. 21st Int. Workshop Active-Matrix Flatpanel Displays and Devices (AM-FPD), 2017, p. 274.
25) Y. H. Hwang, S.-J. Seo, J.-H. Jeon, and B.-S. Bae, Electrochem. Solid-State Lett. **15**, H91 (2012).
26) G. H. Kim, H. S. Kim, H. S. Shin, B. D. Ahn, K. H. Kim, and H. J. Kim, Thin Solid Films **517**, 4007 (2009).
27) H. S. Shin, B. D. Ahn, K. H. Kim, J.-S. Park, and H. J. Kim, Thin Solid Films **517**, 6349 (2009).
28) S. W. Tsao, T. C. Chang, S. Y. Huang, M. C. Chen, S. C. Chen, C. T. Tsai, Y. J. Kuo, Y. C. Chen, and W. C. Wu, Solid-State Electron. **54**, 1497 (2010).
29) S.-Y. Huang, T.-C. Chang, S. Y. Huang, M.-C. Chen, S.-W. Tsao, S.-C. Chen, C.-T. Tsai, and H.-P. Lo, Solid-State Electron. **61**, 96 (2011).
30) E.-J. Yun, J. W. Jung, B. C. Lee, and M. Jung, Surf. Coatings Technol. **205**, 5130 (2011).
31) R. M. Ferrizz, R. J. Gorte, and J. M. Vohs, Catal. Lett. **82**, 123 (2002).
32) C. Kittel, *Introduction to Solid State Physics* (Wiley, New York, 1986) 6th ed., p. 76.
33) S. S. Zumdahl, *Chemical Principles* (Houghton Mifflin, Boston, MA, 2009) 6th ed., p. A23.